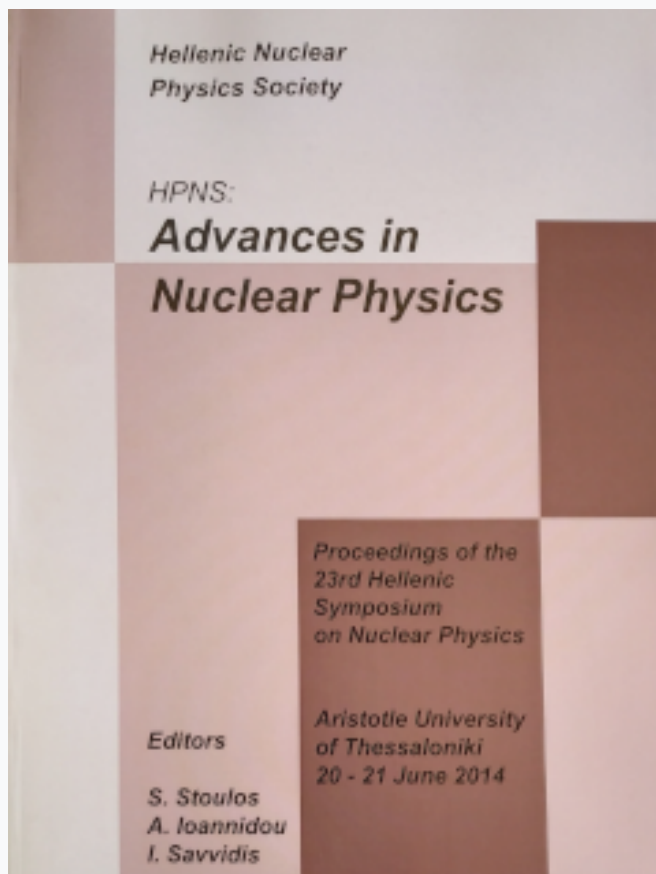


## HNPS Advances in Nuclear Physics

Vol 22 (2014)

HNPS2014



### Microscopic Calculations of Low and Medium Energy Fission with the CoMD (Constrained Molecular Dynamics) Model

N. Vonta, G. A. Souliotis, A. Bonasera, M. Veselsky

doi: [10.12681/hnps.1932](https://doi.org/10.12681/hnps.1932)

#### To cite this article:

Vonta, N., Souliotis, G. A., Bonasera, A., & Veselsky, M. (2019). Microscopic Calculations of Low and Medium Energy Fission with the CoMD (Constrained Molecular Dynamics) Model. *HNPS Advances in Nuclear Physics*, 22, 67–73. <https://doi.org/10.12681/hnps.1932>

# Microscopic Calculations of Low and Medium Energy Fission with the CoMD (Constrained Molecular Dynamics) Model

N. Vonta<sup>1</sup>, G.A. Souliotis<sup>1</sup>, A. Bonasera<sup>2</sup>, M. Veselsky<sup>3</sup>

<sup>1</sup>*Lab. of Physical Chemistry, Dep. of Chemistry, University of Athens, 15771, Greece.*

<sup>2</sup>*Cyclotron Institute, Texas A&M University, College Station, Texas, USA.*

<sup>3</sup>*Institute of Physics, Slovak Academy of Sciences, Bratislava, Slovakia.*

---

## Abstract

The investigation of the mechanism of nuclear fission is a topic of current experimental and theoretical interest. In this work, we initiated a systematic study of low and intermediate energy fission calculations using the Constrained Molecular Dynamics (CoMD) code. The code implements an effective interaction with a soft isoscalar part and with several forms of the density dependence of the nucleon symmetry potential. In addition, CoMD imposes a constraint in the phase space occupation for each nucleon restoring the Pauli principle at each time step of the evolution of the nuclear system. Proper choice of the surface parameter of the effective interaction has been made to describe fission. In this work, we present CoMD calculations for several proton-included fission reactions at low and intermediate energy and compare them with recent experimental data. We found that the CoMD code is able to describe the complicated many-body dynamics of the fission process especially for intermediate and higher-energy fission reactions. Proper adjustment of the parameters of the effective interaction and further improvements of the code are necessary to achieve a satisfactory quantitative description of low-energy fission where shell effects play a definitive role.

---

## Introduction

The microscopic description of the mechanism of nuclear fission is a topic of intense nuclear research. Understanding of nuclear fission, apart from the theoretical many-body point of view, is of practical importance for energy generation, isotope production, as well as for the transmutation of nuclear waste. Furthermore, nuclear fission is essentially the process that defines the upper limit of the periodic table of the elements and plays a vital role in the production of heavy elements via the astrophysical r-process [1]. Motivated by the present state of affairs regarding fission research, we initiated a systematic study of low and intermediate energy fission using the Constrained Molecular Dynamics (CoMD) code of A. Bonasera and M. Papa [4,5].

## Theoretical Framework

The Constrained Molecular Dynamics (CoMD) code is based on the general approach of molecular dynamics as applied to nuclear systems [2,3]. The nucleons are assumed to be localized gaussian wavepackets in coordinate and momentum space. A simplified effective nucleon-nucleon interaction is implemented with a nuclear-matter compressibility of  $K=200$  (soft EOS) with several forms of the density dependence of the nucleon-nucleon symmetry potential. In addition, a constraint is imposed in the phase space occupation for each nucleon, restoring the Pauli principle at each time step of the collision. Proper choice of the surface parameter of the effective interaction was made to describe fission.

In the calculations of the present work, the CoMD code was used essentially with its standard parameters. The soft density-dependent isoscalar potential was chosen ( $K=200$ ). For the isovector part, several forms of the density dependence of the nucleon-nucleon symmetry potential are implemented. Two of them were used in the present work: the “standard” symmetry potential [red (solid) lines] and the “soft” symmetry potential [blue (dotted) lines] in the figures that follow. These forms correspond to a dependence of the symmetry potential on the 1 and the 1/2 power of the density, respectively. The surface term of the potential was set to zero to describe fission. For a given reaction, a total of approximately 5000 events were collected. For each event, the impact parameter of the collision was chosen in the range  $b = 0-6$  fm, following a triangular distribution. Each event was followed up to 15000 fm/c and the phase space coordinates were registered every 50 fm/c. At each time step, fragments were recognized with the minimum spanning tree method [4,5], and their properties were reported. Thus, information on the evolution of the fissioning system and the properties of the resulting fission fragments were obtained. In this way, the moment of scission of the deformed heavy nucleus could be determined. We allowed 2000 fm/c after scission for the nascent fission fragments to deexcite and we reported and analyzed their properties.

## Results and Comparisons

Motivated by the present bibliography concerning the nuclear fission of uranium isotopes, we performed calculations related to the proton induced fission of  $^{235}\text{U}$ , at 10 MeV, 30 MeV, 60 eV and 100 MeV. Moreover, calculations have been performed for the proton induced fission of  $^{238}\text{U}$ , at 100 MeV and 660 MeV energies.

In Fig. 1, in the experimental data of the reaction  $p$  (27 MeV) +  $^{232}\text{Th}$ , we observe the asymmetric nature of the fission of  $^{232}\text{Th}$ . In contrast, the CoMD calculations result in a symmetric distribution with a flat top. The main reason is that the nucleon-nucleon interaction in the CoMD model does not include spin dependence, and thus the resulting mean field potential has no spin-orbit contribution. Consequently, the model cannot reproduce the correct shell effects necessary to describe the asymmetric low-energy fission of  $^{232}\text{Th}$ .

When the proton energy increases (Fig. 2), it is expected that the shell effects will fade and the fissioning system will preferentially undergo symmetric fission. The mass yields for the same reaction at proton energy 63 MeV is presented. The experimental mass yield becomes more symmetric at this energy and the calculated yield curve is in better agreement with the data

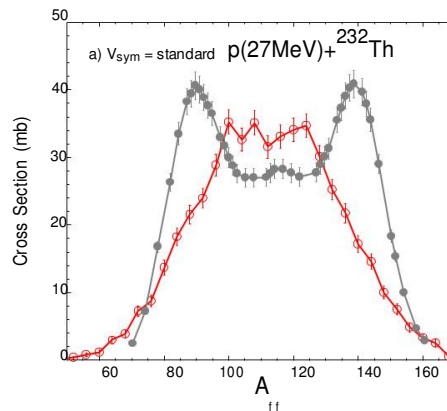


Fig. 1. Normalized mass distributions (cross sections) of fission fragments from  $p$  (27 MeV) +  $^{232}\text{Th}$ . Full points (grey): experimental data [6]. Open points: CoMD calculations with the standard symmetry potential.

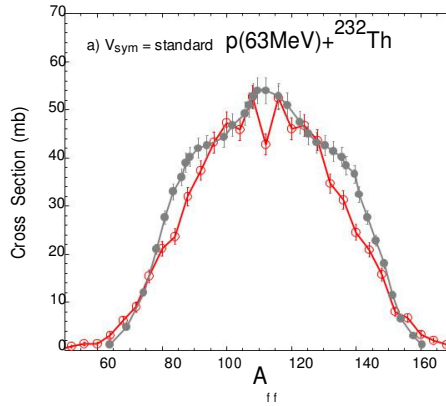


Fig. 2. Normalized mass distributions (cross sections) of fission fragments from p (63 MeV) +  $^{232}\text{Th}$ . Full points (grey): experimental data [6]. Open points: CoMD calculations with the standard symmetry potential.

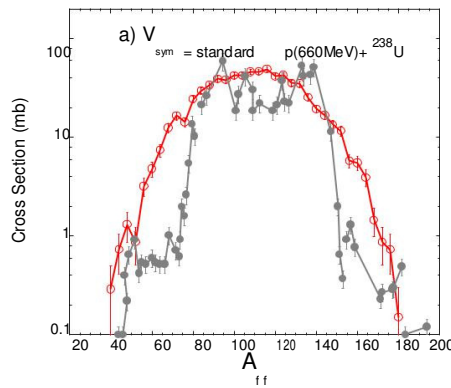


Fig. 3. Normalized mass distributions (cross sections) of fission fragments from p (660 MeV) +  $^{238}\text{U}$ . Full points (grey): experimental data [8]{10}. Open points: CoMD calculations with the standard symmetry potential.

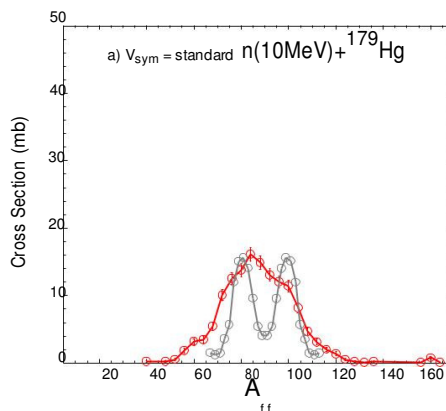


Fig. 4. Normalized mass distributions (cross sections) of fission fragments from n (10 MeV) +  $^{179}\text{Hg}$ . Full points (grey): experimental data [11,12]. Open points: CoMD calculations with the standard symmetry potential.

In Fig. 3, the mass distribution of proton induced fission of  $^{238}\text{U}$  at 660 MeV is presented and it is in good agreement with the experimental data [8]{10}. We observe, mostly the

symmetric fission mode, due to the vanishing of the shell effects. Moreover, the calculations are able to describe satisfactorily the superasymmetric fission, which has been experimentally seen at fission fragment masses  $\sim 40 - 80$  and  $\sim 140 - 180$ . In Fig. 4, we present the mass distribution for the neutron induced fission of  $^{180}\text{Hg}$  at 10 MeV. The experimental data [11,12] are compared with the calculations. The work of [12] introduces a new type of asymmetric fission in proton-rich nuclei. It is related to the exotic process of  $\beta$ -delayed fission of  $^{180}\text{Tl}$ . The experimental data represent the fission fragment mass distribution of the  $\beta$ -decay daughter nucleus  $^{180}\text{Hg}$ , which is asymmetric. The asymmetric nature is surprising due to the fact that the nucleus  $^{180}\text{Tl}$  is expected to be divided into two fragments of  $^{90}\text{Zr}$ , with magic number of neutrons  $N=50$  and semi-magic of protons  $Z=40$ , which are supposed to be more stable. The data of [11] are in arbitrary units and in order to be compared with the calculations, an appropriate scaling of the distribution has been made (multiplication factor 180). In the experimental data, the asymmetric nature of the fission is obvious. On the contrary, the CoMD calculations cannot describe correctly the shell effects and for this reason, the distribution is symmetric.

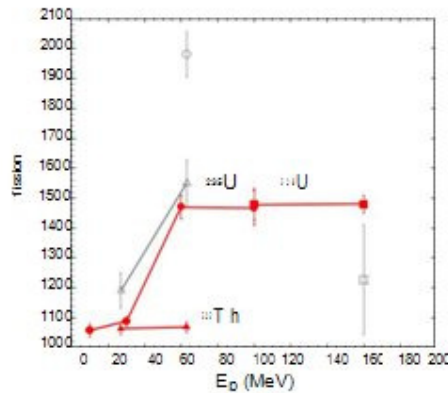


Fig. 5. Calculated total fission cross section with respect to proton energy  $E_p$ . The CoMD calculations are carried out with the standard symmetry potential and are shown with full (red) symbols connected with full (red) lines. The reactions are indicated as follows: triangles: p (27, 63 MeV) +  $^{232}\text{Th}$ , circles: p (10, 30, 60, 100 MeV) +  $^{235}\text{U}$ , squares: p (100, 660 MeV) +  $^{238}\text{U}$ . Some experimental data are shown with open symbols as follows: triangles: p (27, 63 MeV) +  $^{232}\text{Th}$  [6], circles: p (60 MeV) +  $^{235}\text{U}$  [7], square: p (660 MeV) +  $^{238}\text{U}$  [9,10]. The point at  $E_p=660$  MeV is displayed at  $E_p=160$  MeV.

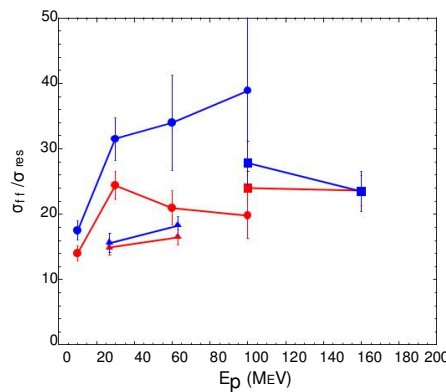


Fig. 6. Calculated ratio of the fission cross section over residue cross section with respect to proton energy. CoMD calculations with the standard symmetry potential are with full (red) symbols connected with full (red) lines. Calculations with the soft symmetry potential are with full (blue) symbols connected with dot-ted (blue) lines. The reactions are indicated as follows: triangles: p (27, 63 MeV) +  $^{232}\text{Th}$ , circles: p (10, 30, 60, 100 MeV) +  $^{235}\text{U}$ , squares: p (100, 660 MeV) +  $^{238}\text{U}$ . The points at  $E_p=660$  MeV are displayed at  $E_p=160$  MeV.

The total fission cross section is presented in Fig. 5 in reference to the various proton energies for the proton induced fission of  $^{232}\text{Th}$ ,  $^{235}\text{U}$  and  $^{238}\text{U}$ . Concerning the fission of thorium, we observe that increasing the excitation energy there is only a slight increase. However, the experimental data show a jump of approximately 30%.

In Fig. 6, we present the correlation between the excitation energy and the ratio of the fission cross section over the residue cross section. For the fission of  $^{232}\text{Th}$  we observe an increase in this ratio towards higher excitation energy. Hence, at 63 MeV beam energy, our calculations show higher probability for fission, in reference to the energy 27 MeV. Moreover, for the fission of the  $^{235}\text{U}$  and  $^{238}\text{U}$ , the probability of getting fission decreases at excitation energies, starting from 30 MeV to 100 MeV and from 100 MeV to 660 MeV respectively. Furthermore, a sensitivity of the calculations concerning the symmetry potential choice is depicted. For the soft potential choice, the aforementioned ratio increases and this means that this choice leads to an increasing probability of getting fission, especially for the proton induced fission of  $^{235}\text{U}$  at various proton energies.

It is very difficult to estimate the fission time from experimental data. Because of the fact that the CoMD is a dynamical microscopic code, we can naturally obtain the dynamical path of the process and therefore determine the fission time. In Fig. 7, the fission time is plotted versus the proton energy of the indicated reactions. We performed the calculations under the restrictions that the fissioning system be a)  $Z=91$ , for  $^{232}\text{Th}$  b)  $Z=93$ , for  $^{235}\text{U}$  and  $^{238}\text{U}$ , which are represented by the open circles, squares and triangles (open symbols).

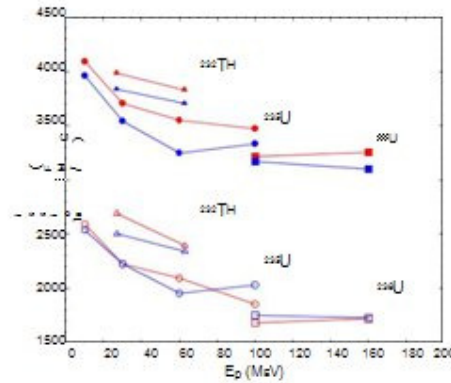


Fig. 7. Calculated fission time with respect to incident proton energy. CoMD calculations with the standard symmetry potential are with (red) symbols connected with full (red) lines. Calculations with the soft symmetry potential are with (blue) symbols connected with dotted (blue) lines. The full symbols (upper half of the figure) are with the full ensemble of the fissioning nuclei, whereas the open symbols (lower half) are with the selection of the fissioning system not to emit any pre-scission protons (see text). The reactions are indicated as follows: triangles:  $p(27, 63 \text{ MeV}) + ^{232}\text{Th}$ , circles:  $p(10, 30, 60, 100 \text{ MeV}) + ^{235}\text{U}$ , squares:  $p(100, 660 \text{ MeV}) + ^{238}\text{U}$ . The points at  $E_p=660 \text{ MeV}$  are displayed at  $E_p=160 \text{ MeV}$ .

Moreover, the closed symbols refer to the CoMD calculations where the full ensemble of the fissioning nuclei is taken into account. For this ensemble, we noticed that the code emits on average two pre-scission protons. The general trend shows that the fission time decreases with the increase of the excitation energy. We observe that the open symbols are lower than the closed ones. The general trend shows that the fission time decreases when the proton energy increases. Additionally, the choice of  $Z$  for the fissioning system leads to a decrease of the fission time. When this choice is made, the total Coulomb

energy is larger (since no pre-scission protons are emitted) and thus, the fissioning system is more fissionable.

## Discussion and Conclusions

In the present work we employed the semi-classical microscopic code CoMD to describe mostly proton induced fission, in a variety of energies on  $^{232}\text{Th}$ ,  $^{235}\text{U}$  and  $^{238}\text{U}$  nuclei. We chose these nuclei because of the availability of recent literature data and because of their significance in current applications of fission. We found that the CoMD code in its present implementation is able to describe fission at higher energies where the shell effects are washed out. We mention that the effective nucleon-nucleon interaction employed in the code has no spin dependence and thus the resulting mean field has no spin-orbit contribution. We are exploring possibilities of adding such a dependence on the potential to give us the ability to adequately describe the characteristics of low energy fission.

We note that the total fission cross sections were rather well reproduced and the ratio of total fission cross sections over residue cross sections appears satisfactory. Interestingly, this ratio shows sensitivity on the choice of the symmetry potential. Concerning the mean total energies and the neutron multiplicities, we mention that they are rather adequately reproduced [13]. Finally, information on the fission time scale is obtained from the present calculations. The obtained fission times show dependence on the excitation energy of the fissioning nucleus, as well as on the choice of the symmetry potential.

In closing, we point out that the CoMD code gives results that are not dependent on the specific dynamics being explored and, thus, offer valuable predictive power for the different modes of fission without adjustable parameters. Consequently, the code can be used for the study of fission of either very neutron-rich or very neutron-deficient nuclei, which have not been studied experimentally to date. Furthermore, this possibility can be exploited to study the fission of very exotic nuclei related to the end point of the r-process, namely the process of fission recycling.

## Acknowledgements

We are thankful to M. Papa for his version of the CoMD code, and to Hua Zheng for his rewritten version of the CoMD. We are also thankful to W. Love-land for his enlightening comments and suggestions on this work. Furthermore, we wish to acknowledge the motivation and recent discussions on experimental aspects of fission with Y.K. Kwon and K. Tshoo of the KOBRA team of RISP (Korea).

## References

- [1] J. Erler et al, Nature 486, 509 (2011).
- [2] A. Bonasera, F. Gulminelli, J. Molitoris, Phys. Rep. 243, 1 (1994).
- [3] J. Aichelin, Phys. Rep. 202, 233 (1991).
- [4] M. Papa et al., Phys. Rev. C 64, 024612 (2001).
- [5] M. Papa et al, J. Comp. Phys. 208, 403 (2005).
- [6] P. Demetriou et al., Phys. Rev. C 82, 054606 (2010).

- [7] M. C. Duijvestijn et al., Phys. Rev. C 64, 014607 (2001).
- [8] A. Deppman et al., Phys. Rev. C 88, 064609 (2013).
- [9] G.S. Karapetyan et al., Phys. Atom. Nucl. C 72, 911 (2009).
- [10] A.R. Balabekyan et al., Phys. Atom. Nucl. C 73, 1814 (2010).
- [11] A.V. Andreev et al., Phys. Rev. C 88, 047604 (2013).
- [12] A.N. Andreyev et al., Phys. Rev. Lett. 105, 252502 (2010)
- [13] N. Vonta, G.A. Souliotis, M. Veselsky, A. Bonasera, Phys. Rev. C submitted (2015).